

Revision 1

Manuscript 8389

The distribution of carbonate in apatite: the environment model

Claude H. Yoder, Kathleen R. Stepien, Robyn N. Dudrick

Department of Chemistry

Franklin and Marshall College

Lancaster PA 17603

Keywords

carbonate apatite, environment model, infrared spectroscopy, NMR spectroscopy

Abstract

The environment model is used to describe the location of carbonate in nine carbonated apatites containing varied percentages of carbonate and Na^+ , K^+ , or NH_4^+ ions. Unlike the traditional model for carbonate substitution, which identifies different locations and orientations of the carbonate ion in the apatite structure, the environment model utilizes the different structural surroundings to describe the different types of carbonate. The A-type carbonate environment is assigned to channels lined only with calcium ions (A-channel configuration = Ca_6) or to channels containing one Na^+ or a vacancy (A'-channel configuration = Ca_5Na or $\text{Ca}_5\Box$), and the B-type carbonate environment is the surroundings of the replaced phosphate ion. The assignments are made by peak-fitting the carbonate asymmetric stretch region (ν_3) of the IR spectrum, following previously published criteria. These assignments lead to the conclusion that

the percentage of channel carbonate (A- and A'-environments) is greater than that of B- type for each of these carbonated apatites. In general, the use of triammonium phosphate as the phosphate source in the synthesis produces apatites with larger amounts of channel carbonate (A- and A'-environments), while the use of sodium-containing phosphate reagents produces smaller amounts of channel carbonate.

The environment model provides explanations for the differences within IR and NMR spectra obtained for apatites containing a range of total carbonate content. The B-type appearance of the carbonate ν_3 region of the IR spectrum is found primarily in apatites containing sodium, which allows increased amounts of carbonation via co-substitution of Na^+ with carbonate and creation of A'-environments with populations equal to that of B-type carbonate. The presence of ammonium or alkali metal salts with cations larger than Na^+ results in the utilization of a charge-balance mechanism that produces vacancies rather than cation substitution in the channel. The carbonated apatites formed with primary utilization of the vacancy mechanism generally contain greater percentages of carbonate in the A-environment and carbonate IR spectra that contain an obvious high frequency peak at about 1550 cm^{-1} . The multiple peaks in the solid state ^{13}C NMR spectra previously observed for carbonated apatite are attributed to substitution in the A-, A'-, and B-environments rather than different stereochemical orientations of the carbonate ion.

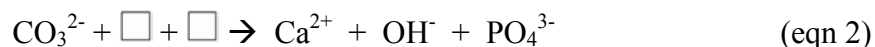
Introduction

The applications of the apatite family of minerals are well known (Rakovan and Pasteris 2015): orthopedic bone and tooth restoration, remediation of heavy metals, fertilizer production, and radioactive waste encapsulation. The use of apatite in bone and tooth restoration often relies on

a close analog of the mineral portion of bones and teeth—carbonated apatite. The structure of this biomaterial (Pasteris 2016) has been studied since the 1950s when it was recognized (McConnel 1952; LeGeros et al. 1968; LeGeros et al. 1969) that the carbonate in apatite can take the place of either phosphate (B-type substitution) in the apatite matrix or hydroxide (A-type substitution) in the apatite channel. B-type substitution was believed to be dominant in bones and teeth and in synthetic apatite prepared in aqueous solution at $T < 100^{\circ}\text{C}$. Figure 1 shows the channel motif that punctuates the nearly close-packed arrangement of calcium and phosphate ions in apatite ($\text{Ca}_{10}(\text{PO}_4)_6(\text{OH})_2$).

Fig 1

When B-type substitution of carbonate occurs, the -3 phosphate ion is replaced by a -2 carbonate ion, which requires a decrease in the positive charge remaining in the apatite matrix. This charge-balance can occur by several mechanisms (De Maeyer et al. 1996; Montel et al. 1981; Pan and Fleet 2002: co-substitution of Na^+ along with carbonate, with the sodium replacing a Ca^{2+} ion in the channel (equation 1), or simultaneous removal of a calcium ion and a hydroxide ion from the channel, leaving vacancies for both ions (equation 2).



When Na^+ is present in sufficiently high concentrations in the synthesis mixture, for example as a counter ion of one of the synthesis reagents, equation 1 represents the balance of charges. Regardless of which mechanism dominates, the channel composition is changed by B-type substitution: co-substitution (equation 1) changes the six channel cations in one unit cell from a configuration of Ca_6 to the configuration Ca_5Na , whereas equation 2 produces vacancies for

hydroxide ions within the channel and calcium ions defining the channel and leads to the configuration $\text{Ca}_5\Box$ (\Box represents a vacancy).

The environment model

When carbonated apatites are prepared in aqueous solution both A- and B-type substitutions occur and, as a result of the B-type substitution, channel carbonate, produced by A-type substitution, can exist in channels that have configurations of Ca_6 , Ca_5Na , $\text{Ca}_5\Box$, Ca_4Na_2 , and so on (Montel et al. 1981). Therefore, a channel carbonate ion may be surrounded by six calcium ions that provide a total of a +12 surrounding charge, by five calcium ions and one sodium ion for a charge of +11, and so on. Because of the difference in the surrounding charge, carbonate ions in different environments have different vibrational frequencies. Fleet (2017) utilized the difference in these channel environments to explain the IR spectrum of apatites synthesized at high temperature and pressure. The channel environment model has also been used to explain the IR spectra of calcium and strontium apatites prepared in aqueous solution (Yoder et al. 2019; Bollmeyer et al. 2019)].

The carbonate asymmetric stretching (ν_3) region of A-type carbonated apatite obtained by high temperature reaction of CO_2 with apatite (Yoder et al. 2019), that of a B-type carbonate, and that of an AB-type carbonated apatite prepared in the present study are shown in Figure 2. Four important features of the IR spectra of carbonated apatites are illustrated in this figure: a) in the ν_3 region there is a doublet for every structurally and environmentally distinct carbonate ion in the apatite structure, b) the doublet for A-type carbonate appears at a higher frequency than that of B-type carbonate, c) the distance ($\Delta\nu$) between the members of the doublets is greater for the

A-type doublet, and d) the appearance of the ν_3 region of an AB carbonated apatite can be estimated by summing the spectra of A- and B-type apatites. In cases where there is more than one type of environment for carbonate, each different carbonate will produce a doublet in the ν_3 region at frequencies that are influenced primarily by the charge experienced by the carbonate ion. The carbonate ion also has a distinctive out-of-plane bending (ν_2) region at about 860-885 cm^{-1} , in which each structurally and environmentally different carbonate ion gives rise to only one band (Figure 3).

Fig 2

Fig 3

Because the frequencies of the bands in each region are often similar for ions in different environments, spectral deconvolution is necessary to obtain more precise information about each region. Careful deconvolution of the ν_3 and ν_2 regions of the carbonate IR spectrum produces a larger number of, mostly, higher frequency bands attributed to channel carbonate ions. For example, Fleet (2017) found evidence for three different channel environments and one B-type environment in apatites prepared at high temperatures and pressures. For carbonated hydroxylapatites prepared in aqueous solution, carbonate ions in both A- (Ca_6) and A' - (Ca_5Na or $\text{Ca}_5\text{□}$) environments have been proposed (Yoder et al. 2019).

The traditional model

The traditional model for the location of carbonate in carbonated apatites was constructed primarily by McConnell (1952) and Wallaeyns (1954) in the early 1950s. The substitution of carbonate for phosphate produces a decrease in the a-axis of the unit cell because of the smaller size of the carbonate ion relative to the phosphate ion (McConnell 1952; LeGeros 1965) When

substitution of carbonate for hydroxide occurs, the a-axis increases presumably due to the larger size of the carbonate ion compared to hydroxide ion (Legeros et al. (1969); Wallaeyns 1954). In the traditional model, IR spectroscopy is also diagnostic for pure A-type carbonated apatite, which produces a doublet centered at about 1504 cm^{-1} (Fig. 2 top), and for pure B-type substitution, with a doublet at 1435 cm^{-1} (Fig. 2 middle). Of course, nearly all carbonated apatites prepared in aqueous solution contain both A- and B-type carbonate (Fig. 2 bottom).

The difference between the two models only becomes obvious when it is recognized that B-type substitution must be accompanied by the charge balance necessary to accompany the replacement of a -3 ion with a -2 ion. The two charge balance mechanisms most often invoked (eqns 1 and 2) produce changes in the configuration of ions in the channel. If there is a carbonate ion in the channel (A-type substitution) the carbonate environment then becomes either Ca_5Na or $\text{Ca}_5\text{□}$ rather than the Ca_6 environment present when no B-type substitution has occurred. These environments have different total charges and can therefore produce, and be recognized by, significant changes in the IR spectrum.

The objectives of the current research are to explore the utility of the environment model for the structure of carbonated apatites, prepared using a variety of reagents, in order to: a) identify the compositional and structural factors that influence the population of carbonate ions in the apatite channel, and b) account for the changes in lattice parameters that occur during incorporation of carbonate. The composition and structures of strontium (Weidner et al. 2015; Bollmeyer et al. 2019), barium (Yoder et al. 2012; Wilt et al. 2014), and lead apatites (Sternlieb et al. 2010; Wilt et al. 2014; Kwasniak-Kominek et al. 2017) have been reported. Understanding this model is

particularly important given the possibility of the greater mobility and biological activity of channel ions relative to those in the apatite matrix (Fleet 2017).

Materials and Methods

Synthesis of apatites

All samples were prepared using Milli-Q deionized water and ACS reagent-grade reagents with purities above 98%. ^{13}C -labeled NaHCO_3 (99% purity) was obtained from Sigma-Aldrich. Triammonium phosphate was obtained from City Chemical Co. (New York). Yields were >90%.

All samples were prepared using one of four synthesis methods, including the one-step (Yoder et al. 2017), direct (Yoder et al. 2017), inverse (Vignoles et al. 1988), and Rey et al. (1989) methods.

One-step method: All reagents (Table 1) were combined in a 125-mL Erlenmeyer flask with a 14/20 outer joint. The calcium reagent for every sample was $\text{Ca}(\text{NO}_3)_2 \cdot 4\text{H}_2\text{O}$, the phosphate reagent was either $(\text{NH}_4)_3\text{PO}_4$ or Na_2HPO_4 , and the carbonate reagent was $\text{NaH}^{13}\text{CO}_3$. About 70 mL of water was added to the flask and the solution was stirred with a magnetic stir bar. The pH was adjusted to 9 with 6M NH_3 . A condenser and thermometer were placed in the outer joint of the flask to monitor the temperature, which was maintained at 80°C using a hot plate.

Table 1

Direct method: A 30-mL carbonate solution of 0.17M NaHCO_3 , 0.17M $\text{NaH}^{13}\text{CO}_3$, 0.25M $(\text{NH}_4)_2\text{CO}_3$, or 0.17M KHCO_3 was placed in the bottom of a 250-mL 14/20 three-neck, round-

bottom flask. This solution was heated to 80°C using a heating mantle and stirred with a magnetic stir bar. One addition funnel contained a 30-mL solution of 0.28M Ca(NO₃)₂·4 H₂O. The second dropping funnel contained 30-mL of 0.17M (NH₄)₃PO₄, 0.17M (NH₄)₂HPO₄, 0.17M NH₄H₂PO₄, 0.17M ¹⁵NH₄H₂PO₄, 0.17M Na₃PO₄, 0.17M Na₂HPO₄, or 0.17M K₃PO₄. The calcium and phosphate solutions were slowly added simultaneously at a rate of about 1 drop per second. The pH was adjusted to 9 with 6M NH₃ before the addition began, after the addition of 10 drops, half-way through the addition, and at the conclusion of the addition.

Inverse method: This method is identical to the direct method, except that the phosphate solution was contained in the round-bottom flask, and the carbonate solution was added using an addition funnel. The solution volumes and reagent molarities were the same for both methods.

Rey et al. (1989) method. A 30-mL solution of 0.28M Ca(NO₃)₂·4 H₂O was stirred magnetically in the bottom of a 250-mL round-bottom flask, and the temperature was maintained at 80°C using a heating mantle. A 30-mL solution of 0.18M (NH₄)₃PO₄ and 0.17M NaH¹³CO₃ was added from an addition funnel at a rate of about one drop per second. The pH was adjusted to 9 with 6M NH₃.

In all four synthesis methods the apatite was digested for 24 hours at a pH of 9 and temperature of 80°C. All samples were then filtered through a glass filter crucible using vacuum, and washed four times with a total of 120-mL of water. Samples were dried in a 120°C oven for 12 hours and then ground with a mortar and pestle before characterization.

Characterization

Products were characterized using X-ray powder diffraction with a PANalytical X'Pert PRO Multipurpose diffractometer Theta-Theta System with Cu-K α radiation ($\lambda = 1.54060 \text{ \AA}$). The samples were prepared on a 10 mm cavity slide and were analyzed using the PANalytical program X'Pert Highscore Plus in a range from 5 to 70° 2 θ using a step size of 0.0167 °/step and a dwell time of 3.34 s/step. All products were free of impurities such as calcium phosphate (Ca₃(PO₄)₂) and calcium carbonate as indicated by XRD analyses. Lattice parameters were obtained with the program UnitCell (Holland and Redfern 1997) using hexagonal symmetry. Results were analyzed by removing peaks indicated as potentially deleterious and uncertainties were determined using the statistical measure sigmafit. The program has been previously found to give good agreement with Rietveld analyses (Bollmeyer et al. 2018).

A Bruker Tensor 37 IR Spectrometer with a Ge ATR mount was used to obtain the IR spectra of products using 256 scans at a resolution of 2 cm⁻¹. The uncertainty in peak positions obtained from multiple scans of the same sample is $\pm 0.1 \text{ cm}^{-1}$. For all samples peak-fitting was performed on spectra not modified by smoothing or base-line correction using Thermo Scientific GRAMS/AI Spectroscopy Software Suite. Peak-fitting of the carbonate asymmetric stretch region (ν_3) was based on the environment model discussed previously. In the case of carbonate ions of less than D_{3h} symmetry, each structurally different ion gives rise to two asymmetric stretch and one out-of-plane bend peaks (Fleet 2015, 2017). The use of Gaussian functions for the carbonate asymmetric stretch region (ν_3) and either Gaussian or Lorentzian functions for the out-of-plane bend region (ν_2) accounted for at least 96% of the spectral intensity for most samples. The average standard error for the peak-fitting was 0.0011. Populations (%) of A-, A'-,

and B-carbonate environments were obtained from band areas assuming that the extinction coefficient for each band was the same.

Elemental composition--weight percent sodium, calcium, phosphorus, and potassium-- was obtained using X-ray fluorescence spectroscopy (XRF) with a Panalytical PW 2404 Vacuum Spectrometer equipped with a 4kW Rh X-ray tube. An anhydrous powder of each sample was prepared by ignition at 1200°C, and then used to prepare a glass disc with one part anhydrous sample material and 9 parts lithium tetraborate. The uncertainty in the determination of the percentages of Ca and P is ± 0.05 %.

Carbonate was determined by combustion analysis by Galbraith laboratories (Knoxville, TN), using combustion at 950 °C. Use of oxygen to enhance combustion in the analyzer produced carbonate percentages similar to those obtained without the use of O₂. The relative error in the carbonate percentage is 5%. Elemental nitrogen was determined by Kjeldahl analysis by Galbraith laboratories (Knoxville, TN).

Solid-state MAS NMR spectra were obtained on an Agilent Unity 500 MHz NMR spectrometer equipped with a 3.2 mm solids probe capable of spin speeds of 24 kHz. ¹³C spectra were obtained at 125.500 MHz using a delay time of 100 sec and referenced to adamantane at 37.4 ppm. Errors in the ¹³C chemical shifts are approximately ± 0.3 ppm.

Results

Syntheses

Each of the apatite samples was identified by XRD as containing only an apatite phase and analyzed by XRF for elemental composition and by combustion analysis for carbonate.

Compositional data are given in Table 2. All four synthetic methods produced the desired apatite, though the slow addition method resulted in samples with somewhat narrower xrd peaks. The use of the inverse and Rey methods produced apatites with very similar xrd and IR patterns to those obtained by the direct method, contrary to previous observations (Vignoles et al. 1988).

Many of the syntheses utilized the reagent labeled as triammonium phosphate ((NH₄)₃PO₄, TAP), obtained from City Chemical Co., which, based on elemental analyses, contains 72.24% PO₄ and 21.14% N. Since the theoretical composition of (NH₄)₃PO₄ is 63.84% PO₄ and 28.20% N whereas for (NH₄)₂HPO₄ the theoretical composition is 71.96% PO₄, 21.23% N this reagent appears to be diammonium hydrogen phosphate. However, in our syntheses, triammonium phosphate (TAP) produced apatites that contained a higher percentage of A-type carbonate than that obtained by use of (NH₄)₂HPO₄. Presumably, TAP decomposes to (NH₄)₂HPO₄. Intriguingly, an X-ray structure determination of triammonium orthophosphate trihydrate shows that it is the ortho phosphate and not (NH₄)₂HPO₄•NH₃(H₂O) (Mootz and Wunderlich 1970).

The compounds synthesized using TAP and other ammonium phosphates contained only small amounts of ammonium ion (0.1 % by Kjeldahl determination), consistent with previous work (Vignoles et al. 1987). The ammonium ion was detected in an apatite synthesized with the ¹⁵N isotopomer of ammonium dihydrogen phosphate by ¹⁵N solid-state NMR spectroscopy after a 3-day acquisition.

Table 2

IR spectra

Figure 4 contains the IR spectra of the carbonate region of KS-136. The two carbonate IR regions-- ν_3 and ν_2 -- were fit with Gaussian peaks following the model (Yoder et al. 2019) that carbonate ions in three different environments are necessary to fit the IR intensities as described above. Although both regions can be fit assuming only two carbonate species, the band widths are unacceptably large and more of the intensity of the overall region is left unfit. Perhaps more importantly, six peaks (three carbonate environments) provide a more satisfying explanation for the overall shape of ν_3 , in particular the “peak” at 1493 cm^{-1} , the low frequency shoulder at about 1350 cm^{-1} , and, in the ν_2 region, the low frequency shoulder.

Fig 4

The peak at 1493 cm^{-1} in the IR spectrum of KS-136 is assigned to the high frequency member of the A' doublet while its low frequency member at 1402 cm^{-1} accounts for the low frequency tail to the ν_3 region. The band in the ν_2 region at 866 cm^{-1} has been the subject of a number of papers, which assign it to A2 carbonate in apatite obtained at high pressure and temperature (Fleet et al. 2011) or to “labile carbonate” (Rey et al. 1989) in apatite synthesized at low temperatures, partly because of its response to maturation and heating. This band, observed in all of the compounds studied here and assigned to the A' environment, is not affected by heating. The shapes of both the ν_3 and ν_2 regions (not shown) of apatite KS-99, similar in its IR spectrum to that of KS-136, were not affected by heating successively for four hours at 200, 400, and 800 °C.

A- vs B-type substitution-- appearance of IR spectra

The ν_3 region of the IR spectrum of KS-136 has a very distinctive shape with a significant A-type peak at about 1550 cm^{-1} and an elongated peak at about 1450 cm^{-1} . These same shapes for the ν_3 region of carbonated apatite have been reported elsewhere (Lee et al. 2007; LeGeros 1981; Elliott et al. 1985) particularly for the products of syntheses that utilized $(\text{NH}_4)_3\text{PO}_4$ (Kunio et al. 2006) or $(\text{NH}_4)_2\text{CO}_3$ (Parthiban et al. 2011) and at low carbonate concentrations (LeGeros et al. 1968; Vignoles et al. 1987, 1988; Nelson and Featherstone 1982). The IR spectrum of human enamel also has a similar carbonate ν_3 region (LeGeros et al. 1968; Elliott et al. 1985). In the present study, apatites KS-117, 129, 136, and 151 all have major “A-type” ν_3 regions of the type illustrated by KS-136. The elongation of the 1450 cm^{-1} peak can be attributed to the overlap of the high frequency member of the B-type doublet with the low frequency member of the A-type doublet.

Apatites such as KS-113, 142, and 143 have a carbonate ν_3 region that does not contain an obvious 1550 cm^{-1} peak (Figure 5) and therefore contain little A-type carbonate. These IR patterns are dominated by two bands that can be assigned, at least partly, to a B-type doublet centered at about 1437 cm^{-1} (Tacker 2007). The lower frequency member of this doublet structure is generally more intense, an observation that can be attributed to overlap of the low frequency members of the B- and A'-doublets. The IR spectrum (Fig. 5) of the carbonate region of KS-143 is typical of apatites often described as having B-type carbonate substitution (El Feki et al. 2000; Apfelbaum et al. 1992; Doi et al. 1982), many of which are associated with the presence of sodium.

Fig 5

The out-of plane bending (ν_2) region of the IR spectrum of KS-136 (Fig. 4 (right)) is typical of dominant A-type carbonate: an A-type band appears at 880 cm^{-1} . Bands at $870\text{-}874\text{ cm}^{-1}$ are generally attributed to B-type carbonate, while bands at $875\text{-}880\text{ cm}^{-1}$ are usually assigned to type A carbonate (Fleet 2017). When one peak is observed, as in KS-143 (Fig. 5(right)), it is generally necessary to use deconvolution to obtain more information about the carbonate environments. The spectral envelopes of KS-136 and KS-143 are shown in Figure 6 to facilitate a comparison of the general features of the carbonate IR regions of “A- “ and “B-type” substituted apatites.

Fig 6

NMR solid state spectra

Solid-state ^{13}C NMR spectra also provide evidence for substantial carbonate in the A and A' channel environments in KS-136 and KS-117 and smaller amounts of A-type carbonate in the apatites KS-143 and KS-113. NMR resonances are sensitive to the surroundings of the nucleus being observed, and consequently each carbonate ion in a different environment should produce a separate resonance. Because of the fairly broad resonances obtained in solid state NMR spectroscopy, the resonances may overlap significantly. In the spectrum of KS-117 two peaks are observed (Figure 7) with the higher frequency (higher chemical shift) peak being considerably broader. Assuming that the widths of the resonances should be similar, it is reasonable to assume that the higher frequency peak contains at least two resonances. Because the chemical shift of A-type carbonate has been observed at 166.5 ppm (Beshah et al. 1990) and at 166.2 ppm (Babonneau 2007) in carbonated apatites prepared at high temperature, the peak at 166.7 ppm in KS-117 and at 165.9 ppm in KS-113 can be assigned to carbonate ions in unit cells that have Ca6 channel (A) environments. The deconvolved resonances at approximately 167-

indicate phosphate ions. Lower color intensity denotes position behind (down the z-axis) layer closest to reader. The channels appear at the corners of the unit cell.

Figure 2. Asymmetric stretching (ν_3) region of the IR spectra of carbonated apatites: Top: A-type carbonate formed in high-temperature reaction of CO_2 with hydroxylapatite. Middle: B-type carbonate (KS-123) formed in aqueous solution. Bottom: AB-type carbonate (KS-126) formed in aqueous solution. Peaks are located at: A- 1546, 1461 cm^{-1} ; B-1455, 1415 cm^{-1} , AB: 1541, 1451, 1410 cm^{-1} . Dashed lines indicate peaks for A-type carbonate (red) and B-type carbonate (blue).

Figure 3. The out-of-plane bending (ν_2) region of the IR spectra of carbonated apatites. Top: A-type carbonate formed in high temperature reaction of CO_2 with hydroxylapatite (Yoder et al., 2019). Middle: AB-type carbonated apatite (KS-142) formed in aqueous solution with apparent dominant B-type. Bottom: AB-type carbonated apatite (KS-126) formed in aqueous solution with dominant A-type. Approximate A-type range = 877-880 cm^{-1} , B-type = 870-876 cm^{-1} . Dashed lines indicate A-type carbonate (red) and B-type carbonate (blue)

Figure 4. The carbonate ν_3 (left) and ν_2 (right) regions of the IR spectrum of KS-136 prepared with TAP and KHCO_3 . The ν_3 peak positions for the high-frequency A-peak and the ν_2 peak position for the A-peak are 1548 and 880 cm^{-1} , respectively.

Figure 5. The carbonate ν_3 (left) and ν_2 (right) regions of the IR spectrum of KS-143, prepared using Na_3PO_4 and NaHCO_3 .

Figure 6. The carbonate ν_3 (left) and ν_2 (right) IR spectral regions of KS-136 and KS-143 expanded to illustrate the general patterns for typical A- (KS-136) and B-substituted (KS-143) carbonated apatites.

Figure 7. The ^{13}C solid state MAS NMR spectrum of KS-117.

Figure 8. a-axial length vs percent A- and A'-type environments.

Tables

Table 1. Conditions for the synthesis of prepared apatites

ID	$\text{CO}_3^{2-}:\text{PO}_4^{3-}$ Reactant Ratio	PO_4^{3-} Reagent	CO_3^{2-} Reagent	Synthesis Method
KS-113	1	Na_2HPO_4	$\text{NaH}^{13}\text{CO}_3$	One-step
KS-117	1	$(\text{NH}_4)_3\text{PO}_4$	$\text{NaH}^{13}\text{CO}_3$	Direct
KS-121	1	$\text{NH}_4\text{H}_2\text{PO}_4$	NaHCO_3	Direct
KS-129	2	$(\text{NH}_4)_3\text{PO}_4$	$(\text{NH}_4)_2\text{CO}_3$	Direct
KS-136	1	$(\text{NH}_4)_3\text{PO}_4$	KHCO_3	Direct
KS-142	1	K_3PO_4	KHCO_3	Direct
KS-143	1	Na_3PO_4	NaHCO_3	Direct
KS-150	1	$(\text{NH}_4)_2\text{HPO}_4$	$\text{NaH}^{13}\text{CO}_3$	Direct
KS-151	0.2	$(\text{NH}_4)_3\text{PO}_4$	$\text{NaH}^{13}\text{CO}_3$	Direct
KS-153	1	$(\text{NH}_4)_3\text{PO}_4$	$\text{NaH}^{13}\text{CO}_3$	Rey
KS-154	1	$(\text{NH}_4)_3\text{PO}_4$	NaHCO_3	Inverse
KS-155	1	$^{15}\text{NH}_4\text{H}_2\text{PO}_4$	NaHCO_3	Direct

Table 2. Compositional data

ID	% CO₃	% Na	Ca/P
KS-113	8.65	1.08	1.70
KS-117	2.5	0.66	1.59
KS-121	5.15	0.48	1.66
KS-129	2.95	0.03	1.65
KS-136	2.95	0.037	1.64
KS-142	8.95	0.19	1.83
KS-143	15.5	2.34	2.0
KS-150	6.05	0.58	1.69
KS-151	2	0.3	1.60

Table 3. Spectroscopic assignments

ID	CO₃²⁻ Environment	IR ν_3		IR ν_2		NMR		Average (IR ν_3 + NMR)
		Position (cm⁻¹)	%	Position (cm⁻¹)	%	Position (ppm)	%	
113*	A	1433, 1497	21	853	28	165.9	26	23.5
	A'	1357, 1458	34	839	21	167.3	32	33
	B	1379, 1409	44	846	51	168.1	42	43
117*	A	1422, 1505	29	853	46	166.7	25	27
	A'	1360, 1450	32	842	14	169.4	34	33
	B	1377, 1414	39	847	39	170.5	41	40
129	A	1463, 1550	25	880	41			25
	A'	1399, 1497	33	866	17			33
	B	1417, 1448	43	873	42			43
130	A	1462, 1544	17	880	41			17
	A'	1398, 1492	30	868	26			30
	B	1416, 1451	53	873	33			53
136	A	1461, 1548	27	880	44			27
	A'	1402, 1493	33	866	14			33
	B	1416, 1447	40	873	42			40
142	A	1471, 1530	11	879	24			11
	A'	1396, 1495	43	866	26			43

143	B	1417, 1453	47	873	50			47
	A	1477, 1533	10	879	29			10
	A'	1399, 1493	50	865	22			50
150*	B	1417, 1453	40	872	49			40
	A	1429, 1499	19	853	35	166.1	13	16
	A'	1363, 1454	39	841	28	168.3	41	40
151*	B	1379, 1409	42	847	38	169.6	46	44
	A	1422, 1506	39	853	48	165.6	15	27
	A'	1362, 1457	27	843	20	168.3	39	33
	B	1380, 1411	34	847	32	169.9	46	40

* contains ^{13}C -labeled carbonate

Table 4. Lattice parameters

Sample ID	a-axis (Å)	c-axis (Å)	Unit cell volume (Å ³)
113	9.39(2)	6.91(1)	527(1)
117	9.424(1)	6.885(2)	529.5(2)
129	9.415(3)	6.899(4)	529.6(4)
136	9.415(2)	6.888(2)	528.8(3)
143	9.395(5)	6.894(6)	527.0(6)
150	9.408(8)	6.888(8)	527.0(8)
151	9.422(3)	6.882((3)	529.1(3)

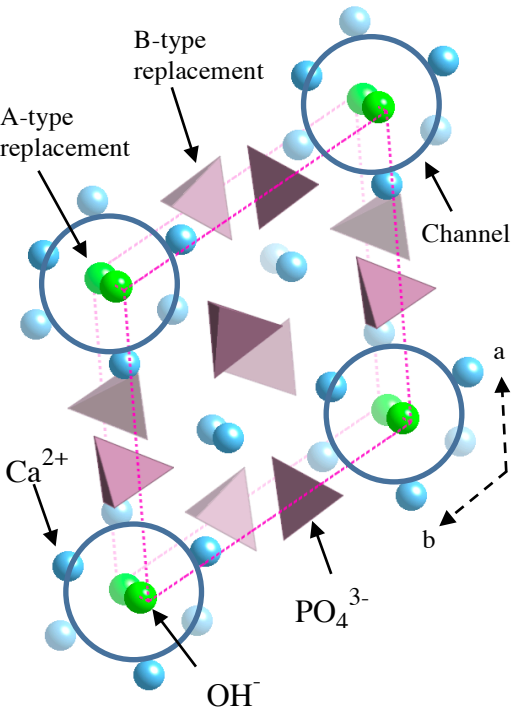
Table 5. Samples with highest and lowest % A-type carbonate environments based on the carbonate IR ν_3 band.

ID (KS-)	Phosphate	% A	% A'	% B	Total % A
Highest % A					
117	T	29	32	39	61
136	T	27	33	40	60
151	T	39	27	34	66
Lowest % A					

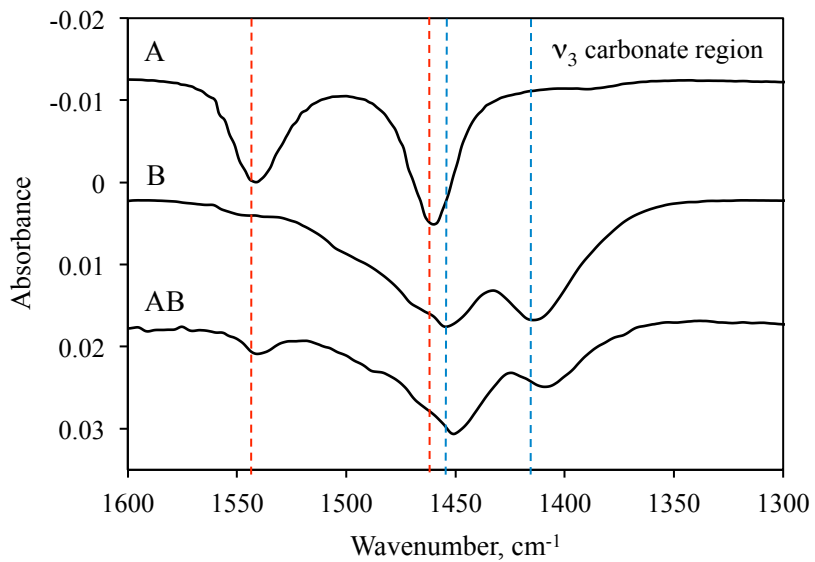
142	$K_2PO_4 / KHCO_3$	10	43	47	53
143	$Na_3PO_4 / NaHCO_3$	10	50	40	60
150	$(NH_4)_2HPO_4$	19	39	42	58

Figures

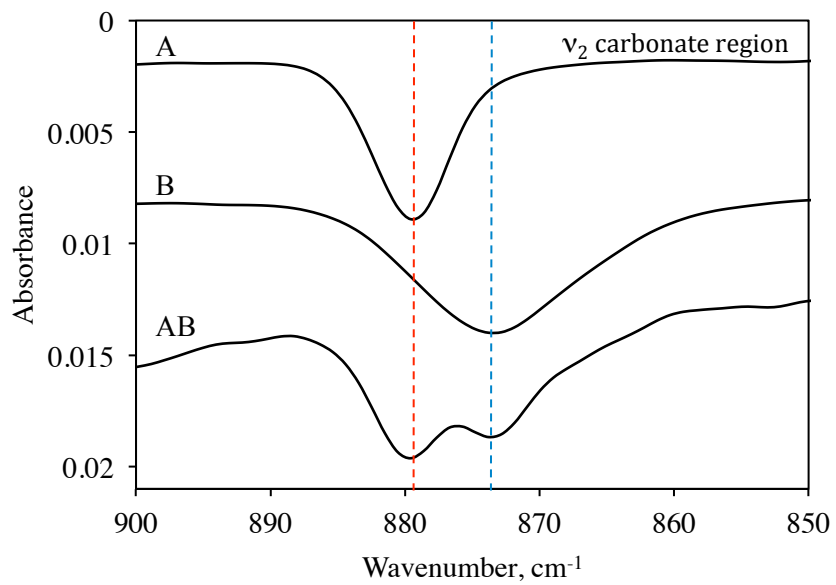
1



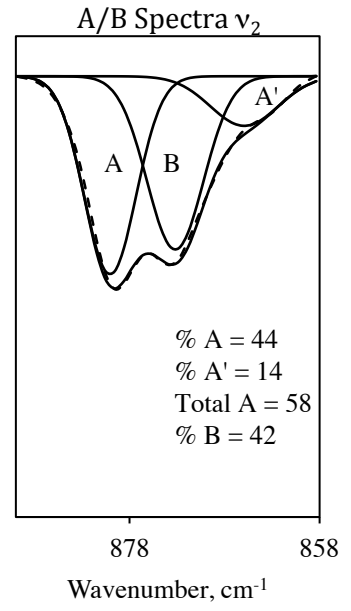
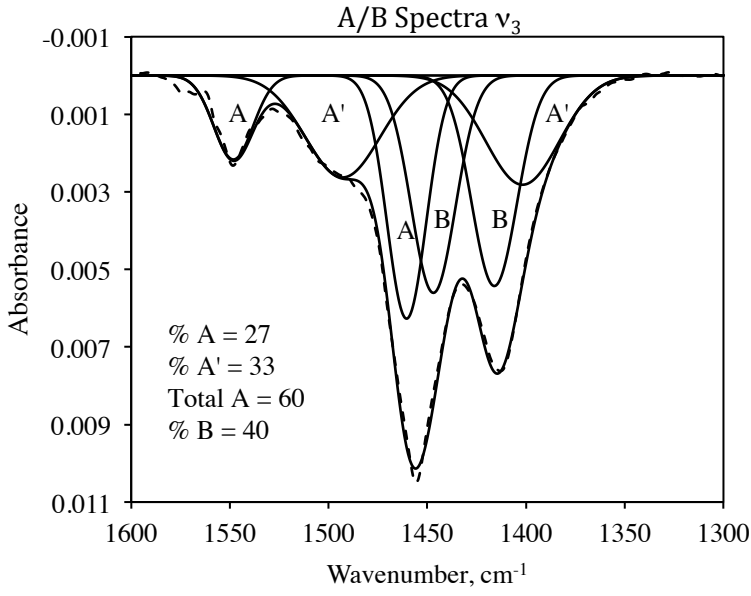
2.



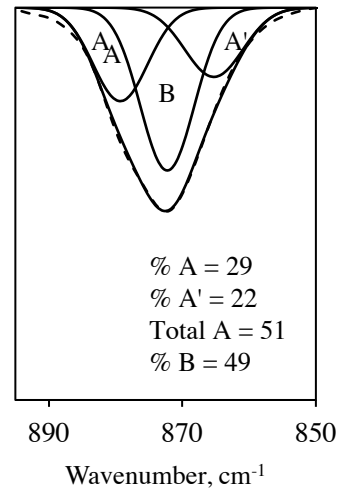
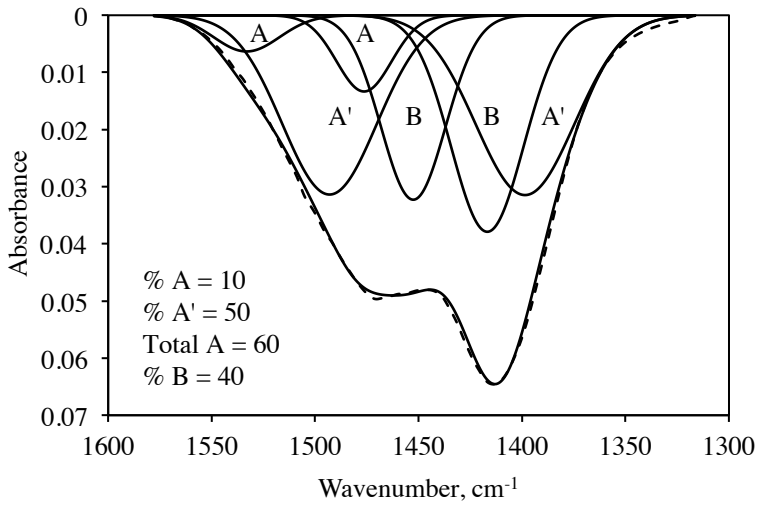
3.



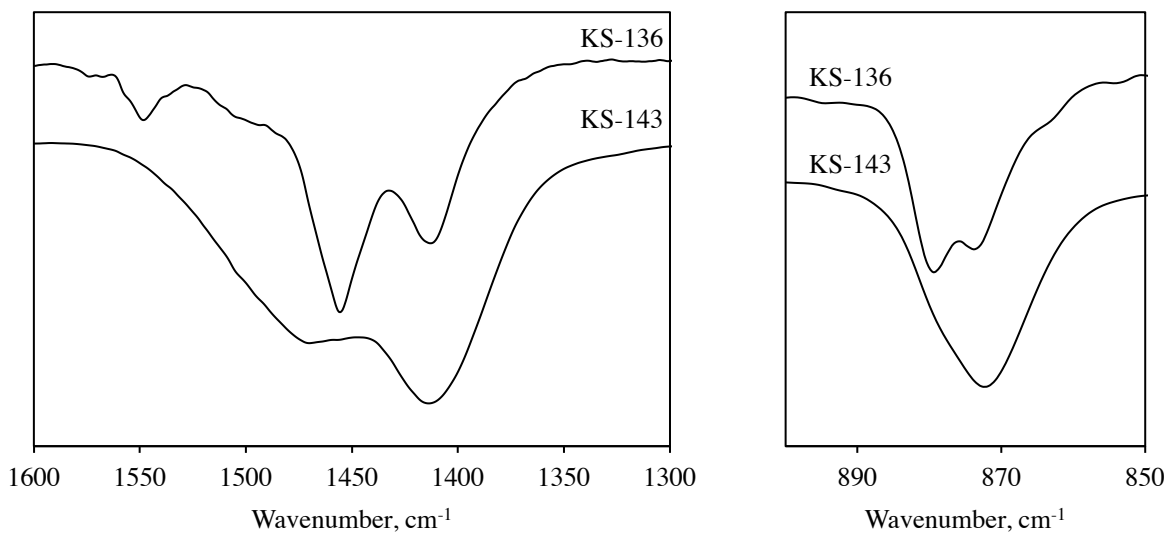
4.



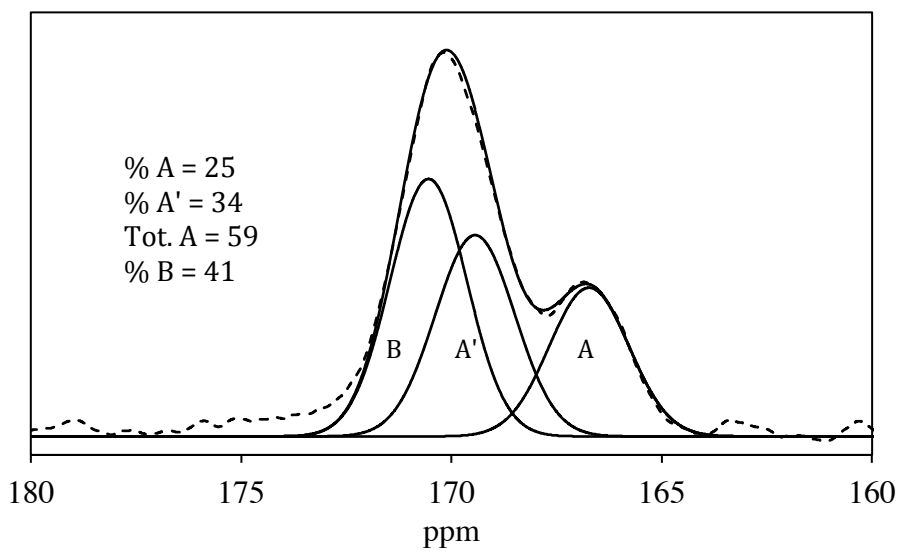
5.



6.



7.



8.

